

## Supporting information

**Synthesis of spin-labeled riboswitch RNAs using convertible nucleosides and DNA-catalyzed RNA ligation**

Lea Büttner, Jan Seikowski, Katarzyna Wawrzyniak, Anne Ochmann, Claudia Höbartner

Research Group Nucleic Acid Chemistry, Max Planck Institute for Biophysical Chemistry,  
Am Fassberg 11, 37077 Göttingen, Germany**Table of contents**

## Sequence information on RNA and DNA oligonucleotides

Tables S1, S2. .... page S2

## Analysis of crude and purified spin-labeled RNAs

Figures S1, S2, S3. .... page S3-4

## Thermal melting analysis

Tables S3, S4, Figures S4, S5 .... page S4-5

## CW-EPR spectra of TEMPO- and proxyl labeled single strands and duplexes

Figure S6. .... page S5

## 9DB1\*-catalyzed ligation of short RNA fragments

Figure S7. .... page S6

## T4 DNA ligase-catalyzed ligation of spin-labeled RNAs

Figure S8. .... page S6

## Characterization of DTT-mediated spin-label reduction

Figure S9. .... page S7

## Ligation of 70-nt SAM-I fragment

Figure S10. .... page S7

## Additional data for full-length SAM-I ligation

Figure S11. .... page S8

<sup>1</sup>H, <sup>13</sup>C and <sup>31</sup>P NMR spectra of new synthetic compounds

Figure S12-19. .... page S9-11

**Table S1.** Unmodified RNAs prepared by solid-phase synthesis or in vitro transcription.

No	5'-Sequence-3'	m.w. calcd.	m.w. found <sup>a</sup>
<b>10</b>	GACGUCGGA	2893.8	2893.1
<b>10'</b>	UCCGACGUC	2790.7	2789.7
<b>11</b>	AAGUCUCAUGUACUA	4720.9	4720.1
<b>11'</b>	UAGUACAUAGAGACUU	4760.9	4760.8
<b>12</b>	GACGUCGGAAGACGUCAGUA	6469.0	6468.5
<b>12'</b>	UACUGACGUCUUCCGACGUC	6279.8	6279.5
<b>13</b>	pppGAUCAAGUGUAGUAUCU	5652.2	5651.4
<b>15</b>	pppGAUGUUCUAGCGCCGGA	5579.2	5578.2
<b>17</b>	pppGACCUCGCAUCGUG	4661.6	4661.9
<b>18'</b>	CACGAUGCGAGGUACUGACGUCUUCCGACGUC	10826.5	10827.2
<b>20</b>	GUUCCGAAAGGAUGGUGGAAUCACCA	8695.3	8694.3
<b>21</b>	pppGAUGCCUUGUAACCGAAAGGGGGAAU	8670.1	8670.5
<b>22</b>	UUCUUAUCAAGAGAAGCA	5724.5	5725.1
<b>23</b>	pppGAGGGACUGGCCGACGAAGCUUCAGCAACCCGUGUAUGGCGAUCAGCCAU	17048.1	n.d. <sup>b</sup>
<b>25</b>	pppGAGGGACUGGCCGACGAAGCUUCAGCAACCCGUGUAUGGCGAUCAGCCAU GACCAAGGUGCUAAAUCAGCAAGCUCGAACAGCUUGGAAGAUAAAGAA	32640.6	n.d. <sup>b</sup>

<sup>a</sup>by ESI-MS. <sup>b</sup> m.w. not determined by ESI-MS, correct length of transcript was confirmed by comparison with length standards on PAGE

**Table S2.** Sequences of 9DB1\* deoxyribozymes

No	5'-Sequence-3'
D1	TACTACACTTGATGGATCATACGGTCGGAGGGGTTTGCCGTTAACCGACGTC
D2	TCCGGCGCTAGAACATGGATCATACGGTCGGAGGGGTTTGCCGTTAACGTACATGAGACTTCC
D3	CACGATGCGAGGTGGATCATACGGTCGGAGGGGTTTGCCGTTAACGTACGTCTTCCGAC
D4	TCGGTTACAAGGCATGGATCATACGGTCGGAGGGGTTTGCCGTTAGGTGATTCCACCATCCTTCGG
D5	GCTTCGTCGGCCAGTCCCTGGATCATACGGTCGGAGGGGTTTGCCGTTAGCTTCTCTGATAAG

Splints for ligation with T4 DNA ligase

S1 GCGCTAGAACATCTAGTACATGACAC for (**11+p15**)

S2 ACGATGCGAGGTCTACTGACGTCTTCCG (for **12+p17**)

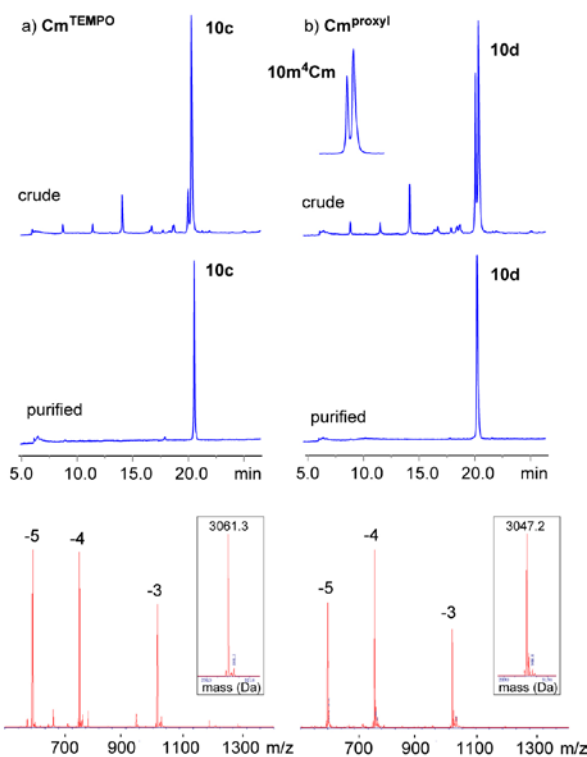


**Figure S1.** Anion exchange HPLC analysis of crude and purified spin-labeled 9-mer RNAs **10**, containing  $\text{Cm}^{\text{TEMPO}}$  and  $\text{Cm}^{\text{proxyl}}$  labels, and characterization by ESI-MS. **10c**: m.w. calcd. 3061.8, found 3061.3; **10d**: m.w. calcd. 3047.8, found 3047.2.

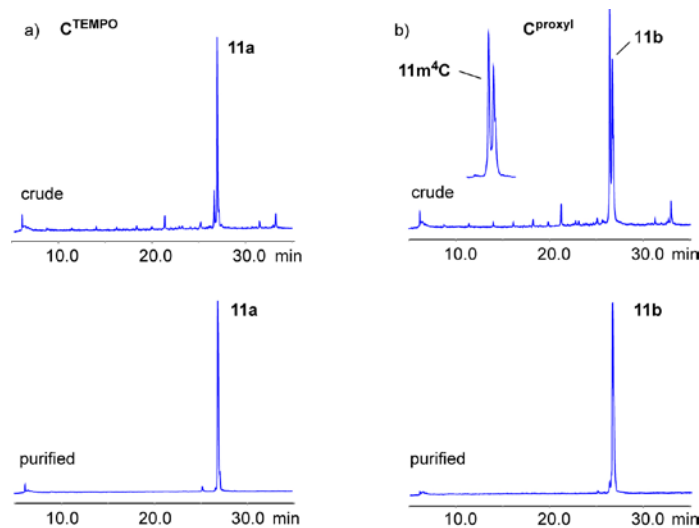


**Figure S2.** Anion exchange HPLC analysis of crude and purified spin-labeled 15-mer RNAs **11a** and **11b**, containing  $\text{C}^{\text{TEMPO}}$  and  $\text{C}^{\text{proxyl}}$  labels.

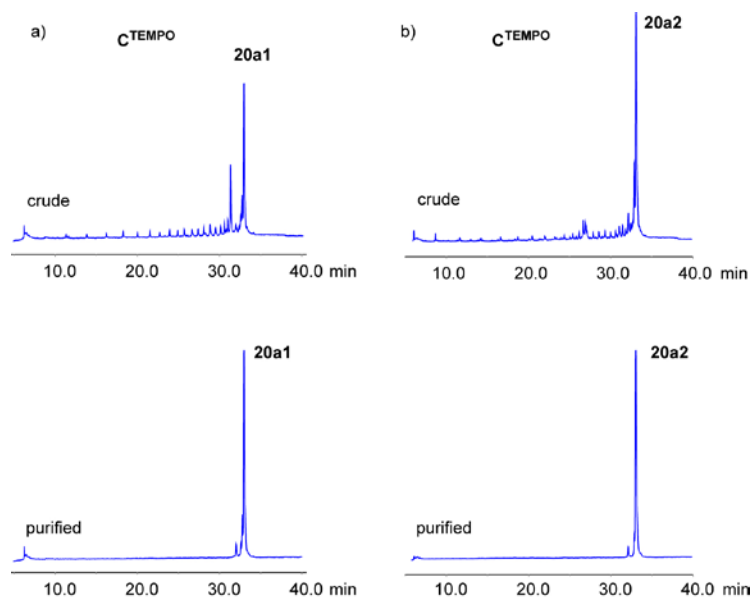


**Figure S3.** Anion exchange HPLC analysis of crude and purified spin-labeled SAM-III riboswitch fragments **20**, containing C<sup>TEMPO</sup> labels.

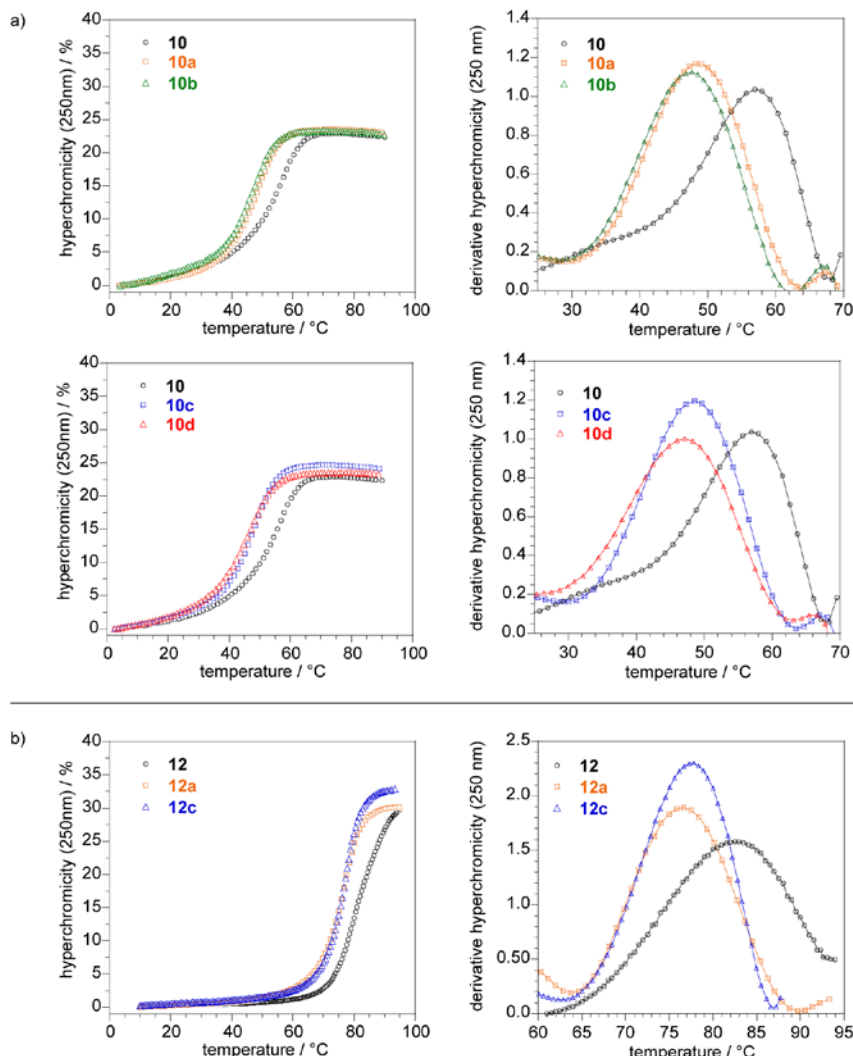


**Figure S4.** Melting curves of a) 9-bp duplexes 10/10'; b) 20-bp duplexes 12/12'. (left: hyperchromicity at 250 nm, right: derivative of hyperchromicity at 250 nm). RNA concentration: 4  $\mu$ M, in 10 mM potassium phosphate, pH 7.0, 150 mM NaCl.

**Table S3.** Concentration-dependent melting temperatures for duplexes **11/11'**.

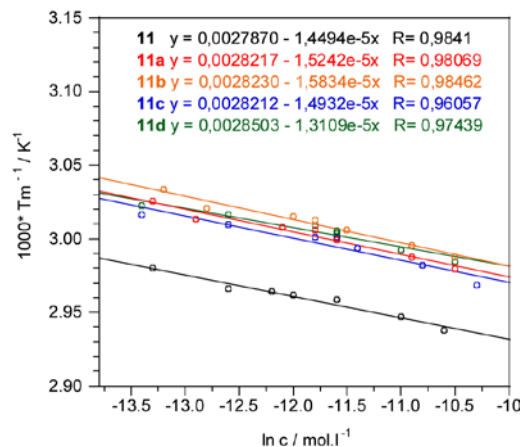
C(11 unmod) conc <sup>a</sup> / $\mu\text{M}$	Tm / °C	C <sup>TEMPO</sup> (11a) conc / $\mu\text{M}$	Tm / °C	C <sup>proxyl</sup> (11b) conc / $\mu\text{M}$	Tm / °C	Cm <sup>TEMPO</sup> (11c) conc / $\mu\text{M}$	Tm / °C	Cm <sup>proxyl</sup> (11d) conc / $\mu\text{M}$	Tm / °C
1.7	62.4	1.7	57.4	1.9	56.5	1.5	58.4	1.6	57.7
3.7	<b>64.0</b>	2.4	<b>58.7</b>	2.8	<b>57.9</b>	3.5	<b>59.1</b>	3.5	<b>58.4</b>
4.9	64.2	5.7	59.3	6.0	58.5	7.5	60.1	7.3	59.2
6.4	64.5	7.3	59.5	7.7	58.8	9.3	60.1	8.9	59.6
9.4	64.8	9.0	60.3	9.9	59.5	10.9	60.9	9.2	59.8
17.1	66.2	17.8	61.6	18.0	60.7	19.8	62.2	16.8	61.0
25.0	67.2	26.4	62.4	26.4	61.6	32.2	63.5	28.6	61.9

<sup>a</sup> concentration calculated from absorbance at 260 nm at Tm. bold values are given in Table 2.

**Table S4.** Thermodynamic parameters for duplexes **11/11'**.

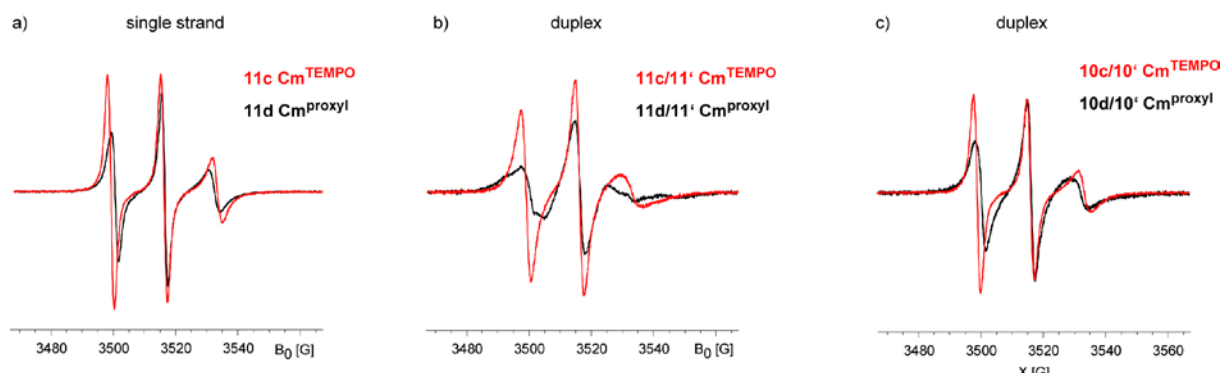
No	label	$\Delta H^\circ$ kcal.mol <sup>-1</sup>	$\Delta S^\circ$ cal.(mol.K) <sup>-1</sup>	$\Delta G_{298}^\circ$ kcal.mol <sup>-1</sup>
<b>11</b>	-	-135	-373	-23.8
<b>11a</b>	C <sup>TEMPO</sup>	-129	-361	-21.4
<b>11b</b>	C <sup>proxyl</sup>	-125	-351	-20.8
<b>11c</b>	Cm <sup>TEMPO</sup>	-133	-373	-22.1
<b>11d</b>	Cm <sup>proxyl</sup>	-148	-419	-23.2

(error:  $\Delta H^\circ$ ,  $\Delta S^\circ$  5-10%,  $\Delta G^\circ$  2-5%)

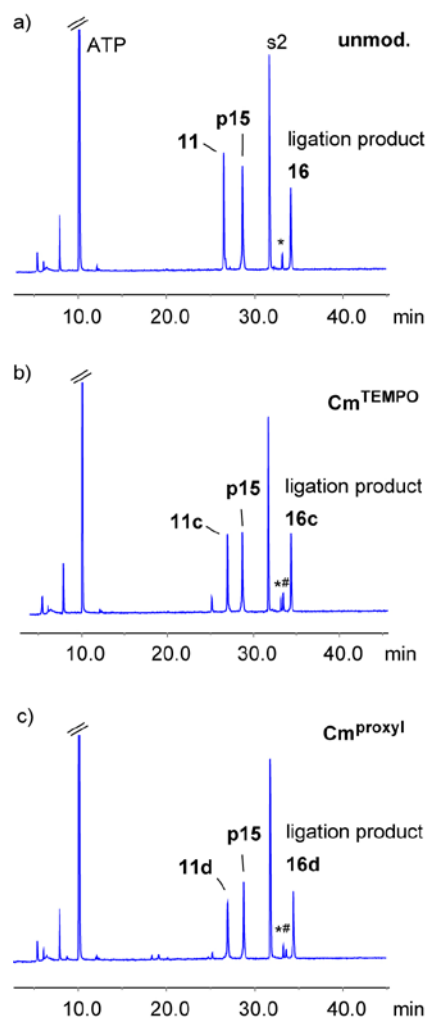
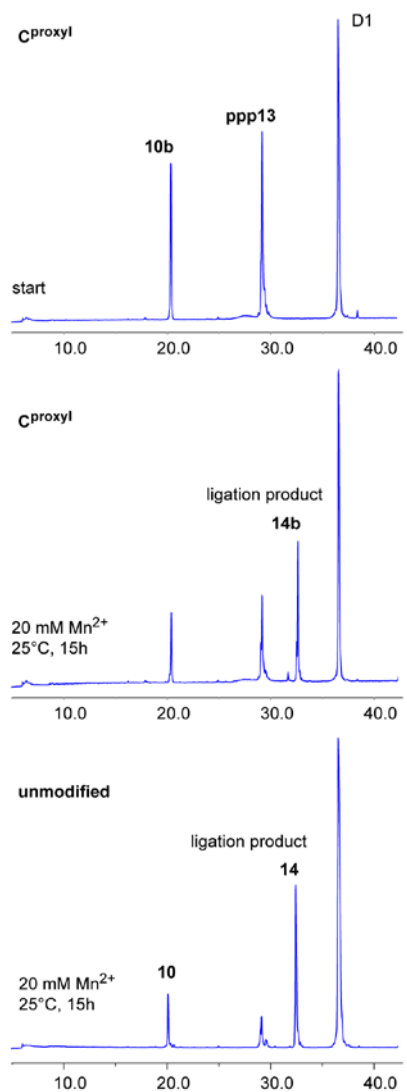


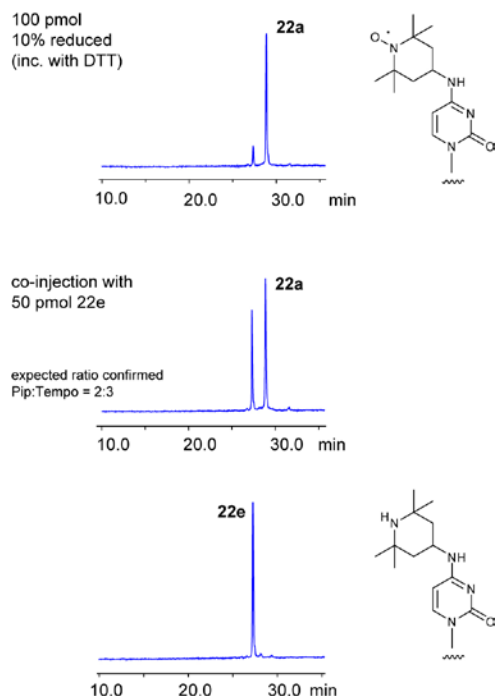
**Figure S5.** Van't Hoff plot for thermal analysis of 15-mer RNA duplexes **11/11'**. Analysis of the bimolecular melting transition of the non-selfcomplementary duplex follows equation (1); thermodynamic parameters are obtained from slope and intercept of the linear regression of the data in the plot of  $\ln(c)$  vs  $1/T_m$ .

$$\text{equation (1): } \frac{1}{T_m} = \frac{R}{\Delta H^\circ} \ln c_{\text{tot}} + \frac{\Delta S^\circ - R \ln 4}{\Delta H^\circ}$$

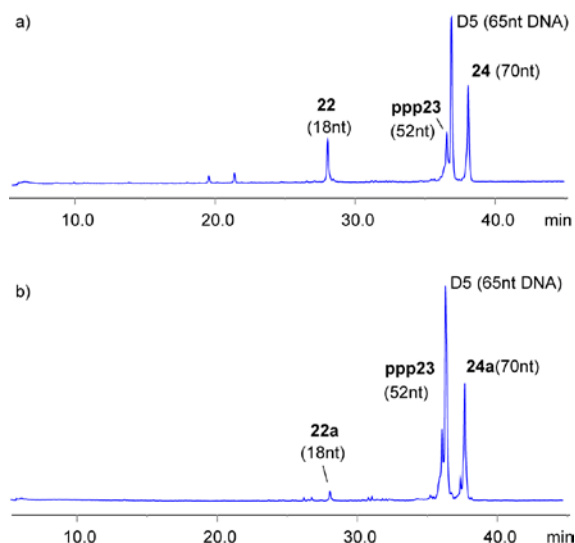


**Figure S6.** Comparison of CW-EPR spectra TEMPO and proxyl-labeled RNAs in single strand and duplex conformations. a) single-strands of RNA **11c** and **11d**; b) duplexes **11c/11'**, **11d/11'**, c) duplexes **10c/10'**, **10d/10'**. 200  $\mu\text{M}$  spin-labeled RNA (1.5 equiv of complementary strand for duplexes), in 2.5 mM potassium phosphate, pH 7.0, 30 mM NaCl, room temperature.

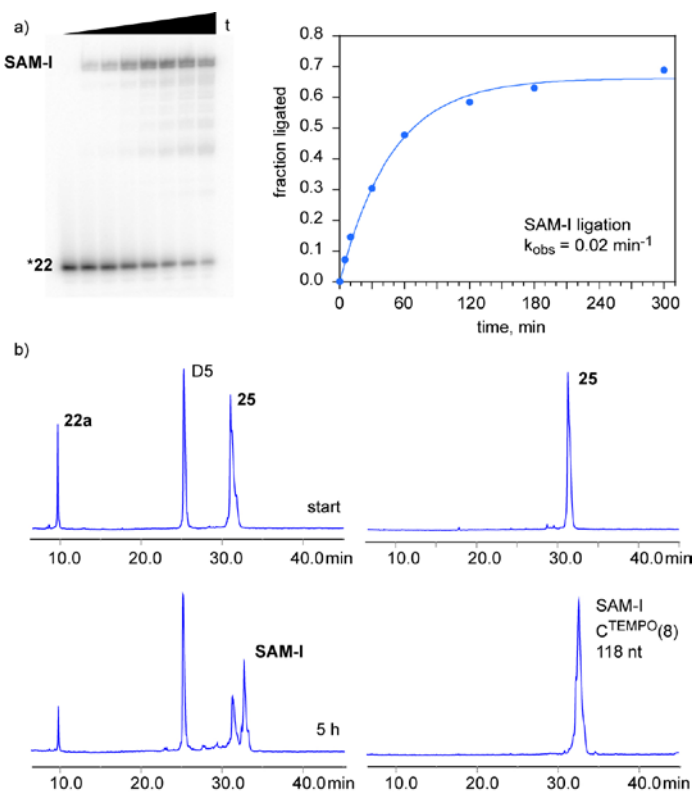




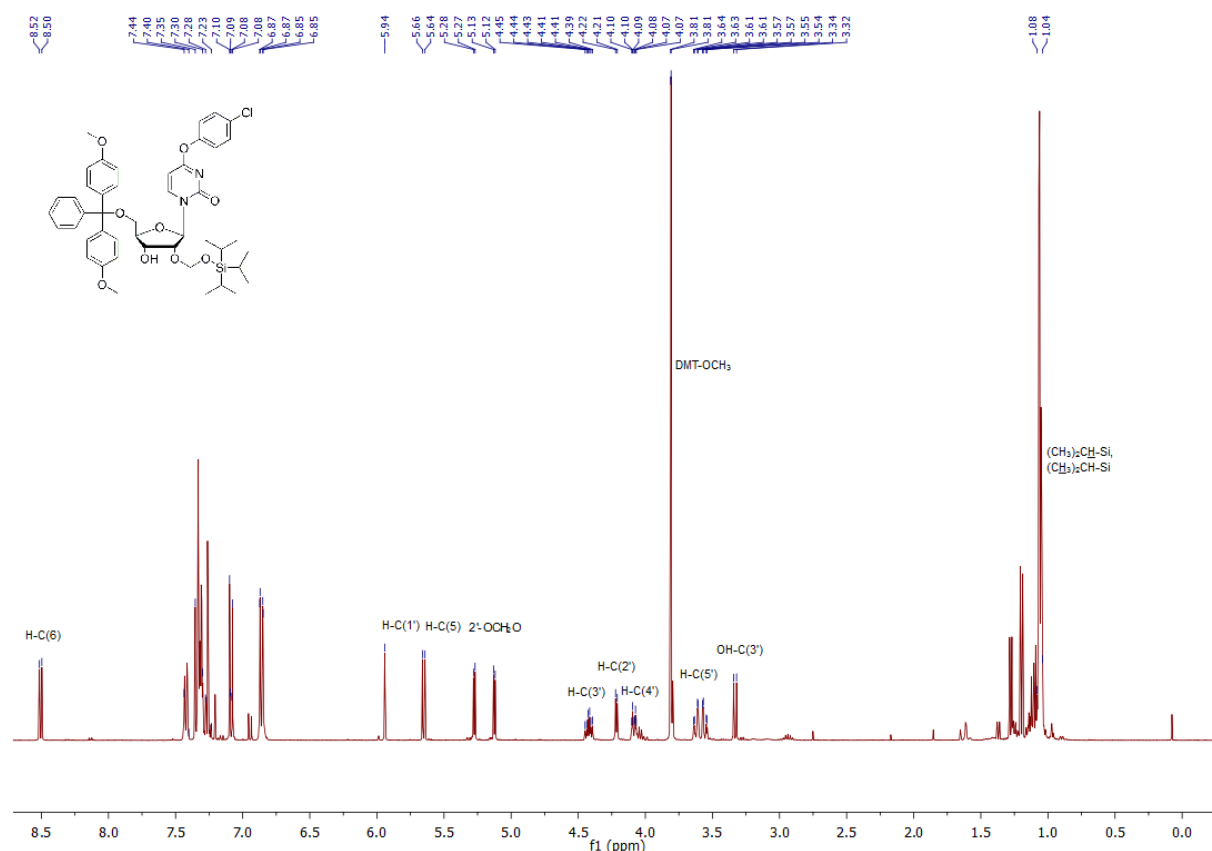
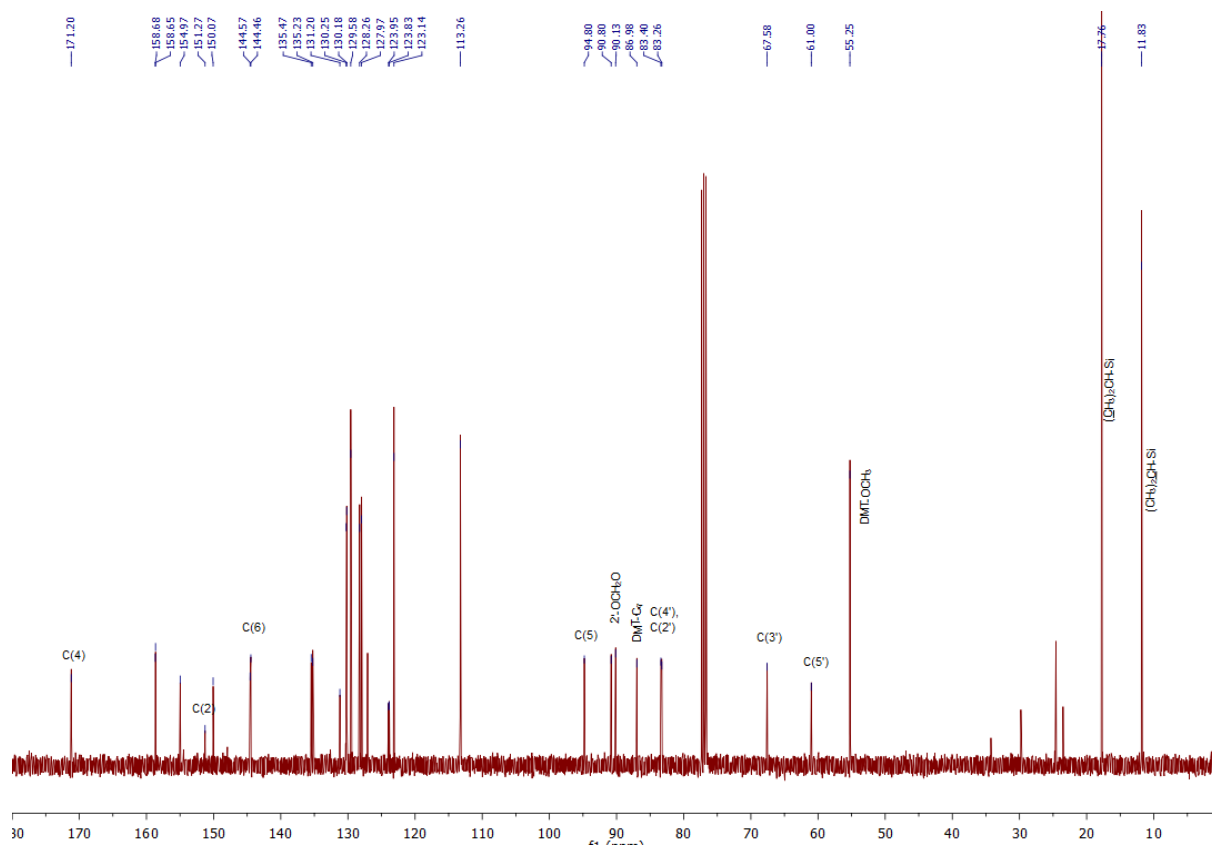
**Figure S9.** HPLC analysis of TEMPO reduction. Comparison with authentic piperidine-substituted RNA.

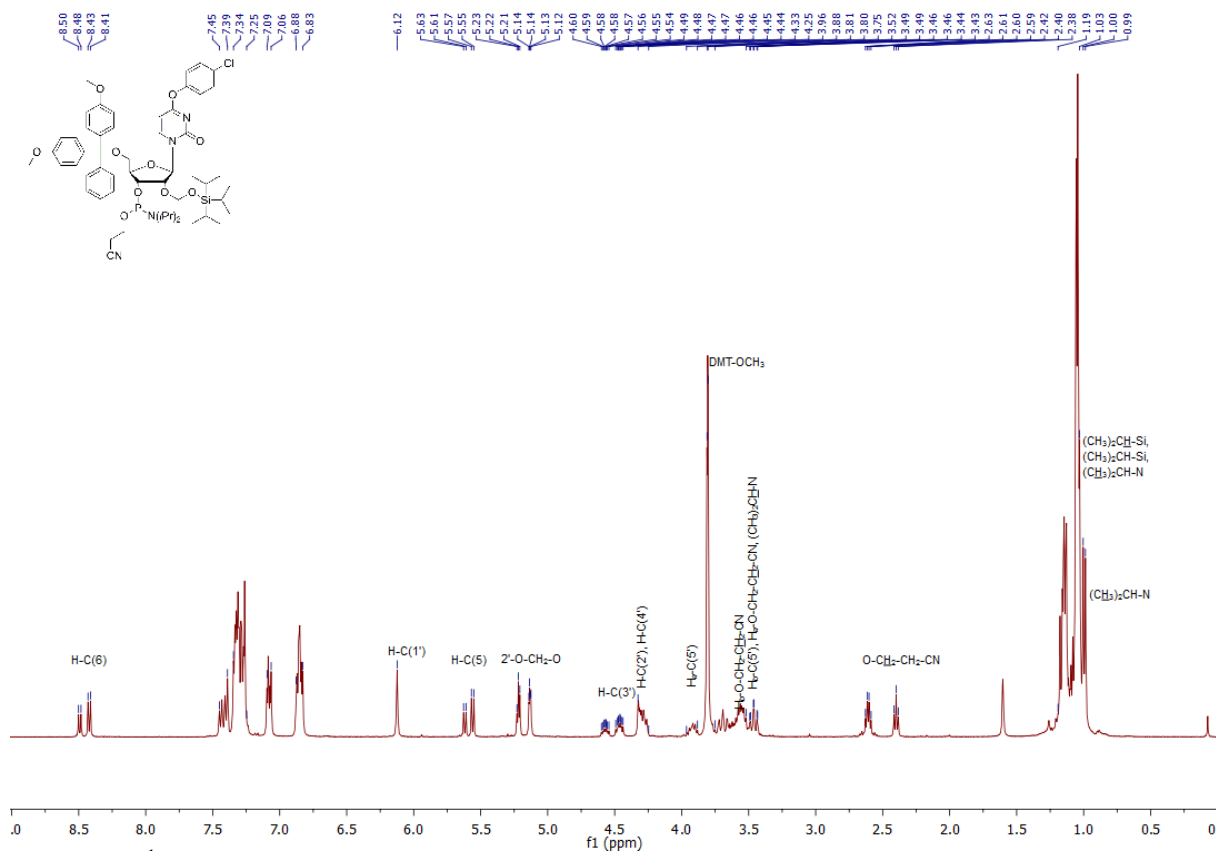
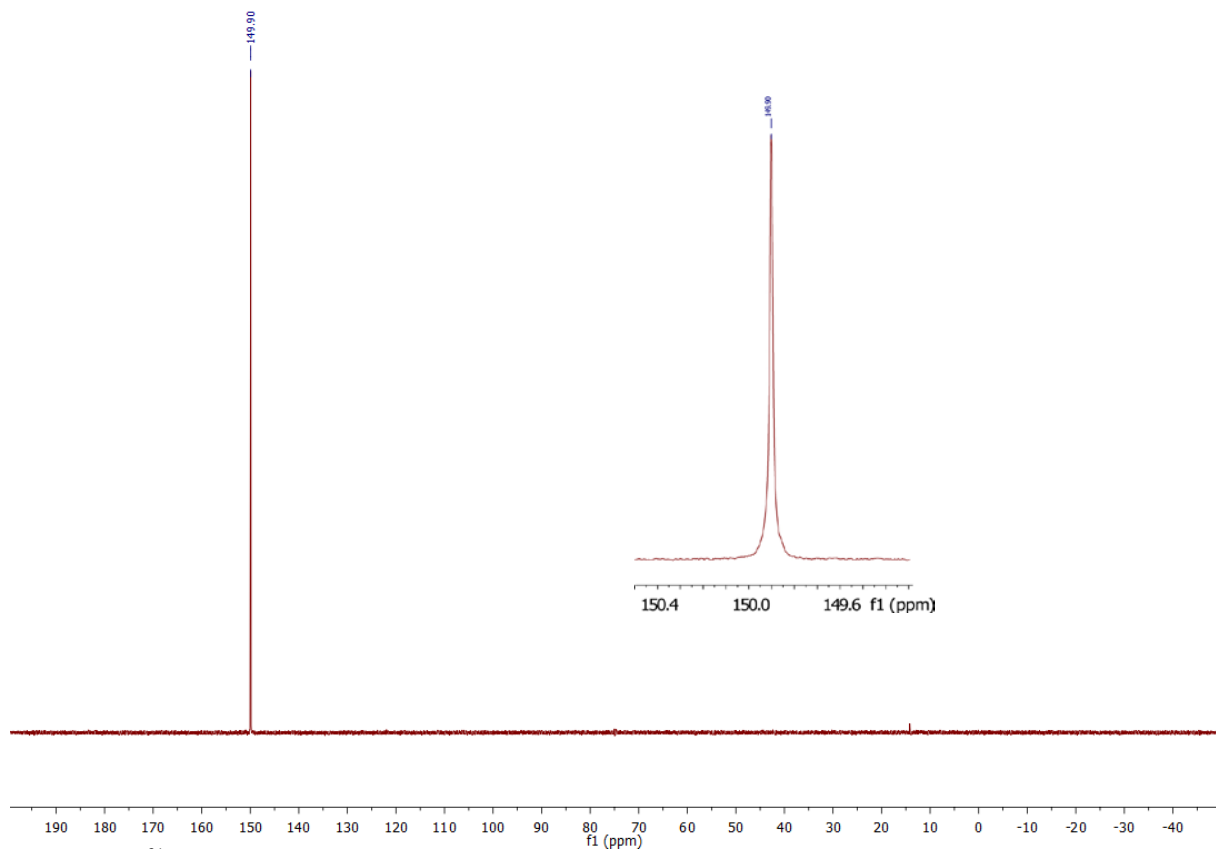


**Figure S10.** HPLC analysis of 9DB1\*-catalyzed ligation of **22/22a** to **23** to generate the first 70 nt of the SAM-I riboswitch sequence. (in b) the transcript **23** was used in 1.5-fold excess over the spin-labeled RNA **22a**)



**Figure S11.** a) Kinetics of 9DB1\*-catalyzed synthesis of SAM-I RNA using 5'-<sup>32</sup>P-labeled **22** and transcript **25**. 10  $\mu$ M RNA, 20 mM MnCl<sub>2</sub>, 50 mM HEPES pH 7.5, 150 mM NaCl, 2 mM KCl, 37°C. b) HPLC analysis of preparative ligation (start and after 5 h). right: analytical HPLC traces of transcript **25** and isolated ligation product, full-length spin-labeled SAM-I RNA (isolated yield: 30%).

**NMR spectra of new compounds****Figure S12.**  $^1\text{H}$  NMR (400 MHz) of compound 3.**Figure S13.**  $^{13}\text{C}$  NMR (100 MHz) of compound 3.

Figure S14.  $^1\text{H}$  NMR (400 MHz) of compound 4.Figure S15.  $^{31}\text{P}$  NMR (162 MHz) of compound 4.

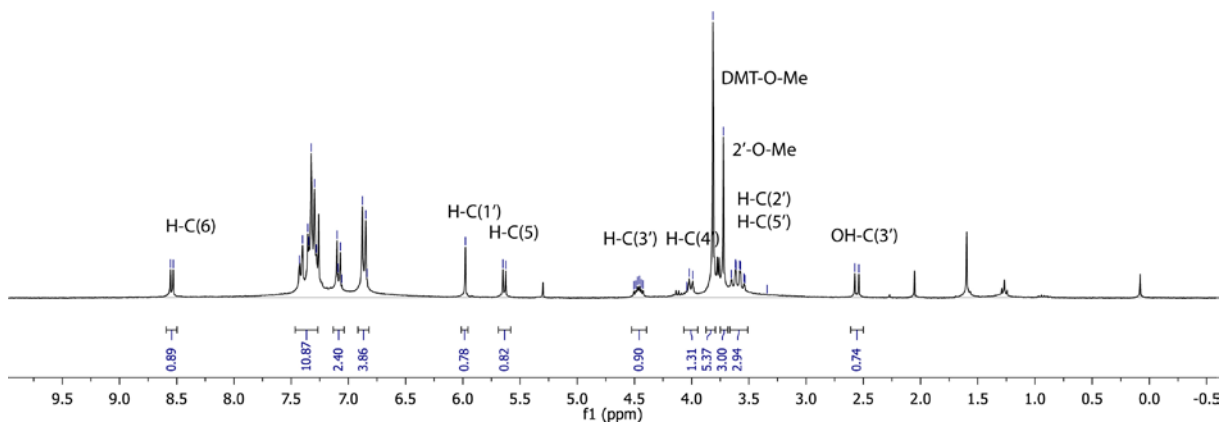
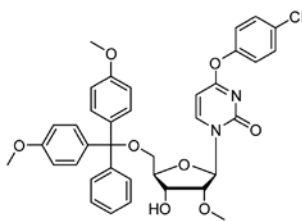


**Figure S16.**  $^1\text{H}$  NMR (400 MHz) of compound **8**.

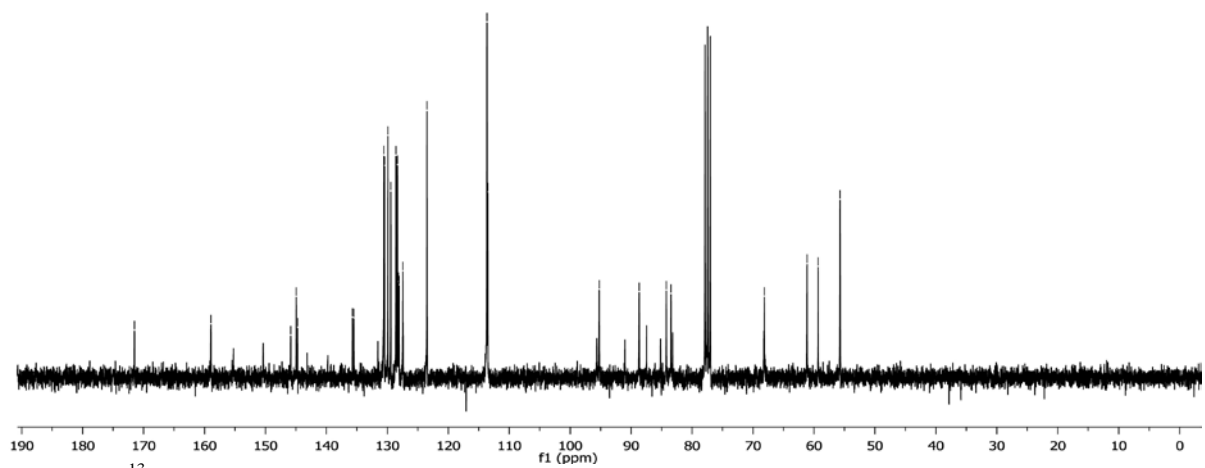
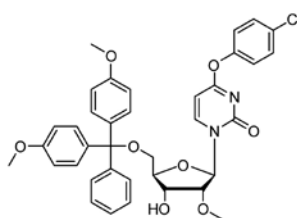
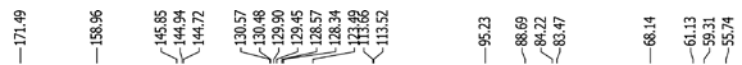


**Figure S17.**  $^{13}\text{C}$  NMR (100 MHz) of compound **8**.

